

Water Resources Research

RESEARCH ARTICLE

10.1029/2023WR036412

Enhanced Hydrologic Connectivity and Solute Dynamics Following Wildfire and Drought in a Contaminated Temperate Peatland Catchment



Key Points:

- Nutrients and base cation streamflow concentrations were elevated following wildfire, and decreased in autumn and spring storm events
- Metals in the catchment showed delayed mobilization, indicating distal headwater source zones rather than proximal to stream sources
- Seasonal re-wetting after drought enhanced catchment hydrologic connectivity, influencing source zone activation and transport

Supporting Information:

Supporting Information may be found in the online version of this article.

Correspondence to:

A. L. Marcotte,
abbey.marcotte@wur.nl

Citation:

Marcotte, A. L., Limpens, J., Nunes, J. P., Howard, B. C., Hurley, A. G., Khamis, K., et al. (2024). Enhanced hydrologic connectivity and solute dynamics following wildfire and drought in a contaminated temperate peatland catchment. *Water Resources Research*, 60, e2023WR036412. <https://doi.org/10.1029/2023WR036412>













Received 3 OCT 2023
Accepted 16 JUN 2024

Author Contributions:

Conceptualization: Abbey L. Marcotte, Juul Limpens, João Pedro Nunes, Kieran Khamis, Stefan Krause, Nicholas Kettridge
Formal analysis: Abbey L. Marcotte
Funding acquisition: Cathelijne R. Stoof, Nicholas Kettridge
Investigation: Ben C. Howard, Alexander G. Hurley, Danny Croghan, Angeliki Kourmouli, Samantha Leader, Tanu Singh, Nicholas Kettridge
Supervision: Juul Limpens, Nicholas Kettridge
Visualization: Abbey L. Marcotte, Juul Limpens

© 2024. The Authors.

This is an open access article under the terms of the [Creative Commons Attribution License](https://creativecommons.org/licenses/by/4.0/), which permits use, distribution and reproduction in any medium, provided the original work is properly cited.

Abbey L. Marcotte¹ , Juul Limpens¹ , João Pedro Nunes² , Ben C. Howard³ , Alexander G. Hurley^{4,5} , Kieran Khamis⁶ , Stefan Krause^{6,7} , Danny Croghan⁸ , Angeliki Kourmouli⁹ , Samantha Leader⁶ , Tanu Singh¹⁰, Cathelijne R. Stoof² , Sami Ullah⁶, and Nicholas Kettridge⁶ 

¹Plant Ecology and Nature Conservation Group, Wageningen University Wageningen, Wageningen, The Netherlands, ²Soil Physics and Land Management Group, Wageningen University, Wageningen, The Netherlands, ³Civil and Environmental Engineering, Imperial College London, London, UK, ⁴Climate Dynamics and Landscape Evolution, GFZ German Research Centre for Geosciences, Potsdam, Germany, ⁵German Council of Experts on Climate Change, Berlin, Germany, ⁶School of Geography, Earth and Environmental Sciences, University of Birmingham, Birmingham, UK, ⁷LEHNA (Laboratoire d'Ecologie des Hydrosystèmes Naturels et Anthropisés), University of Lyon, Villeurbanne, France, ⁸Ecology and Genetics Research Unit, University of Oulu, Oulu, Finland, ⁹Lancaster Environment Centre, Lancaster University, Lancaster, UK, ¹⁰Jacobs UK Limited, Bristol, UK

Abstract Intact peatlands provide hydrological ecosystem services, such as regulating water regimes and immobilizing pollutants within catchments. Climate change impacts including drought and wildfire may impair their functioning, potentially impacting ecosystem service delivery. Here we investigate stream water quality changes following the combined impacts of a summer drought and wildfire in a peat-dominated catchment in the UK during 2018. The study catchment stores legacy pollutants (i.e., metals) due to past industrial activity, thus making it particularly susceptible to pollutant release during wildfires. We quantified changes in water chemistry during five storm events over a 9-month period following the wildfire. Concentration-discharge (C-Q) relationships for nine solutes were analyzed to explore changes in activation and connectivity of solute source zones. Hysteresis and flushing indices of C-Q responses further described solute dynamics during storm events. We found that most nutrient and base cation concentrations in the stream discharge were highest in the immediate post-fire storm events and decreased during subsequent autumn and spring storms. Metal concentrations increased during autumn and spring storms, indicating delayed mobilization from within-peat or distal headwater sources. Our findings suggest that seasonal re-wetting and hydrologic connectivity following disturbance influenced solute source zone activation and transport in the study catchment. Water quality responses associated with wildfire and drought were primarily observed in the months following the wildfire, suggesting mobilization of pollutants peaks shortly after fire. Our results contribute to a critical understanding of the future of water quality risks in temperate peatland catchments subject to disturbances exacerbated by climate change.

Plain Language Summary Peatlands are defined by their accumulated organic matter, providing valuable natural services such as storing carbon, and regulating climate, water quality and runoff. Such capability may be reduced when peatlands are impacted by extreme wildfires and droughts. We studied impacts of a severe wildfire and drought on stream water quality in a peatland catchment in the UK, within a region that may be more frequently impacted by these events in the future due to changing climate. This peatland also stores pollutants (namely metals emitted and retained during the industrial revolution), further enhancing risks to drinking water quality. We determined how the wildfire affected instream chemistry post-fire, and how nutrients and metals moved through the catchment. We found that levels of nutrients in the stream flow increased immediately after the wildfire, followed by a decrease with time. However, the levels of metals increased during the following autumn and spring. This suggests that metals were released later and came from different parts of the catchment compared to the nutrients. Our results show that following the fire, the way water flowed through the catchment played an important role in how substances were transported. The impacts on water quality were most pronounced in the first months post-wildfire and seemed to be short-lived.

Writing – original draft: Abbey L. Marcotte

Writing – review & editing:

Juul Limpens, João Pedro Nunes, Ben C. Howard, Alexander G. Hurley, Kieran Khamis, Stefan Krause, Danny Croghan, Angeliki Kourmouli, Samantha Leader, Tanu Singh, Cathelijne R. Stoof, Sami Ullah, Nicholas Kettridge

1. Introduction

Intact healthy peatlands are an essential component of global freshwater resources, storing approximately 10% of global freshwater (Xu et al., 2018). At a regional scale, intact peatlands can mitigate downstream flooding by attenuating flow via surface runoff and buffer downstream water quality by retaining nutrients and anthropogenic pollutants in vegetation and peat (Bindler, 2006; Shuttleworth et al., 2019). However, these services are compromised and become disservices when peatlands become directly or indirectly degraded by land-use change and disturbances such as wildfire and drought (Wilkinson et al., 2023). These disturbances can cause enhanced erosion (Rothwell et al., 2005) and export of pollutants such as metals (McCarter et al., 2023; Rothwell, Evans, & Allott, 2007; Rothwell, Evans, Daniels, & Allott, 2007; Shuttleworth et al., 2015, 2017), nutrients and other contaminants into waterways (Bladon et al., 2014; Paul et al., 2022).

Severe drought conditions and wildfire occurrence are projected to increase in temperate regions due to climate change (Albertson et al., 2010; Flannigan et al., 2009; Perry et al., 2022). While much research has focussed on quantifying water quality impacts in regions that are historically susceptible to wildfires, such as south-eastern Australia, the Mediterranean or western US (Hampton et al., 2022; Rust et al., 2019; Smith et al., 2011), important aspects of wildfire impacts on water quality in historically less-fire prone regions (i.e., northern Europe) have received far less attention. Given that peatlands in these regions are often receivers and sinks of industrial and atmospherically derived pollutants (Miszczak et al., 2020; Rothwell, Evans, & Allott, 2007; Rothwell, Evans, Daniels, & Allott, 2007; Shotbolt et al., 2006), there is a critical need to understand how disturbances such as wildfires release and mobilize legacy pollutants stored in the peat profile (McCarter et al., 2023).

Dry catchment conditions can impact hydrologic functioning by lowering water table and disconnecting certain flow paths to the streamflow network (van Meerveld et al., 2019). Both drought and wildfires can cause hydrophobic soil conditions (Moore et al., 2017; Wu et al., 2020), which may induce changes in surface and subsurface flow patterns (Moody et al., 2013; Paul et al., 2022), for example, by inducing preferential flow of subsurface paths or saturated areas. These disturbances are also known to influence stream water chemistry by altering nutrient and heavy metal loads (Granath et al., 2021; Smith et al., 2011), both due to creation and alteration of water quality parameters as well as alteration of flow paths and saturated areas that contribute to the stream (Nunes et al., 2018). However, our understanding of interactions between wildfire, drought and water quality are limited in temperate peatlands, particularly in relation to movement of solutes and particulates, because responses likely differ compared to well-studied fire-prone areas due to varying geomorphology and hydrological functioning of peatlands.

Hydrological flow in healthy peatlands is generally conceptualized by two hydrologically important horizons, with a discontinuity of hydraulic conductivity between the two (Ivanov, 1981). The acrotelm is the uppermost functional layer—ca. 0–30 cm deep—where much of the movement of water and transfer of nutrients occurs (Holden & Burt, 2003). The acrotelm may swell and shrink with water availability, thus altering storage and conductivity as water table depth changes. The layer below, the catotelm, consists of older, more decomposed peat with very low horizontal conductivity, keeping the layer fully saturated. The depth-dependent hydraulic conductivity of the acrotelm and the low hydraulic conductivity of the catotelm below can result in short lag times between peak rainfall and peak stream discharge when water tables are close to the surface, but longer lag times when water tables drop (Evans et al., 1999) thus attenuating peak flow. This regulating capacity is strongly related to the thickness of the acrotelm, with thinner acrotelms leading to progressive loss of water flow regulation. For peatlands on slopes, such as blanket peatlands, acrotelms can be thin or discontinuous leading to more flashy hydrographs with large storm peaks due to rapid transfer of water from the hillslopes to the stream channel. Dominating runoff processes from the hillslopes then tend to be overland flow and near- to sub-surface flow either through macropores or naturally occurring soil pipes (Jones, 1981). Spatio-temporal heterogeneity in runoff processes are difficult to resolve because they are influenced by several factors such as antecedent moisture, precipitation intensity, topography and vegetation (Edokpa et al., 2022; Jones, 1981). Additionally, the nature and concentrations of pollutants may also differ between edaphoclimatic regions (Nunes et al., 2018; Paul et al., 2022), which causes impacts of wildfire in temperate peatland catchments to be concerning. Therefore it is crucial to understand the mechanisms underlying solute mobilization and transport through peatland catchments following disturbances to better understand future water quality risks in these regions.

Here we explored the combined impacts of severe drought and wildfire on stream water quality and contaminant mobilisation after the 2018 Stalybridge Moor, UK wildfire (commonly referred to as the Saddleworth Moor

wildfire) that occurred in a temperate peatland contaminated with legacy pollutants. We aimed to identify controls on the activation of solute source zones, mobilisation patterns and transport pathways under different wetness conditions within the disturbed catchment following successive rain storm events. Specifically, we ask the questions: (a) how do severe drought and wildfire impact the hydrological and biogeochemical responses in a heavily contaminated temperate peatland; and (b) what are the mechanisms underlying solute mobilisation and transport in the study catchment following drought and wildfire disturbances?

2. Materials and Methods

2.1. Study Site Description

The study catchment is located within an upland blanket peatland east of Manchester, England (Figure 1a). Much of the area has been heavily impacted by industrial pollution since the beginning of the industrial revolution due to its downwind proximity to industrial towns, notably Manchester and Oldham, and studies in the region indicate that legacy pollutants—such as Pb, Cu, Cd, Zn, and Ni—are stored in the peat profile as a result (e.g., Rothwell, Evans, & Allott, 2007; Rothwell, Evans, Daniels, & Allott, 2007). The study catchment drains an area of 1.8 km², feeding into the Cowbury reservoir (Figure 1b). The reservoir is not used for public water supply, thus it was not subject post fire water quality mitigation efforts. Average annual temperature—recorded at a nearby weather station—is 6.9°C (years 2004–2013) with a warmest month July (13.2°C) and coldest month February (1.6°C) (Clay & Evans, 2017). The recorded mean annual precipitation is ~1,300 mm, ranging from average monthly precipitation of 71–149 mm (Clay & Evans, 2017).

The upland blanket peat catchment is underlain by interbedded sandstones and shales of the Millstone Grit series (Bower, 1961). The catchment consists of strongly sloping areas near the main channel and flatter peat plateaus in the headwaters (Figure 1a), and has an altitudinal range of 251–497 m above sea level. Peat is thicker in the headwaters overlaying a thin layer of clay and rocky outcrops. The peat is highly decomposed with discontinuous shallow acrotelm and has a gradient shifting to shallower organic soils in the stronger sloping areas near the main outlet stream. The stream is a second order stream that drains peat gullies higher in the landscape. The network of gullies dissect the landscape and are eroded down to bedrock in many areas. This is especially evident in areas closer to the stream outlet where the stream cuts into the valley exposing Millstone Grit strata.

Vegetation in the headwaters and on the upper slopes is dominated by heather (*Calluna vulgaris*), cotton grass (*Eriophorum vaginatum*), with interspersed patches of crowberry (*Empetrum nigrum*) and bilberry (*Vaccinium myrtillus*). Bracken (*Pteridium aquilinum*) is found on stronger sloping areas and in patches around the lower reaches of the stream. *Sphagnum* spp. occurs in wetter areas throughout the catchment, notably near gullies and the stream. Few small Silver birch (*Betula pendula*) are present in the riparian area around the stream.

On 24 June 2018 a wildfire broke out over Stalybridge Moor and lasted for approximately 3 weeks and was declared extinguished on 18 July. The fire was one of the largest wildfires in the UK in recent decades (Graham et al., 2020), burning the entire study catchment and a total area of ~18 km². Summer 2018 was one of the warmest recorded in the UK (since records began in 1884). June rainfall totals across parts of central England were less than ~30% of average summer rainfall (1981–2010) (Kendon et al., 2019) causing exceptionally dry and hot weather conditions at the time of the wildfire. A burn severity analysis of the study catchment, following the methodology and classification of Chafer et al. (2016) and Keeley (2009), showed that stronger sloping areas near the streams had highest burn severity, followed by high severity in the headwaters with patches of moderate and low burn severity (Figures 1c–1e).

2.2. Catchment-Wide Monitoring

We established a catchment-wide monitoring network in response to the wildfire event. Instrumentation of the catchment was 13 days after ignition and prior to the first rain storm event, aiming to monitor stream flow and water quality indicators (i.e., a range of elements and variables, turbidity and pH) at the catchment outlet (WQ in Figure 1b). In the study we focused on turbidity, dissolved organic carbon (DOC), sulfate (SO₄²⁻), calcium (Ca), aluminum (Al), lead (Pb), sodium (Na), copper (Cu) and zinc (Zn), which is explained in Section 3.2.1. Dipwells and stilling wells were also installed at different locations along the hillslope to capture spatio-temporal variations in gully stage level ($n = 2$) and water table depth ($n = 7$) (WT1 and WT4 in Figure 1b).

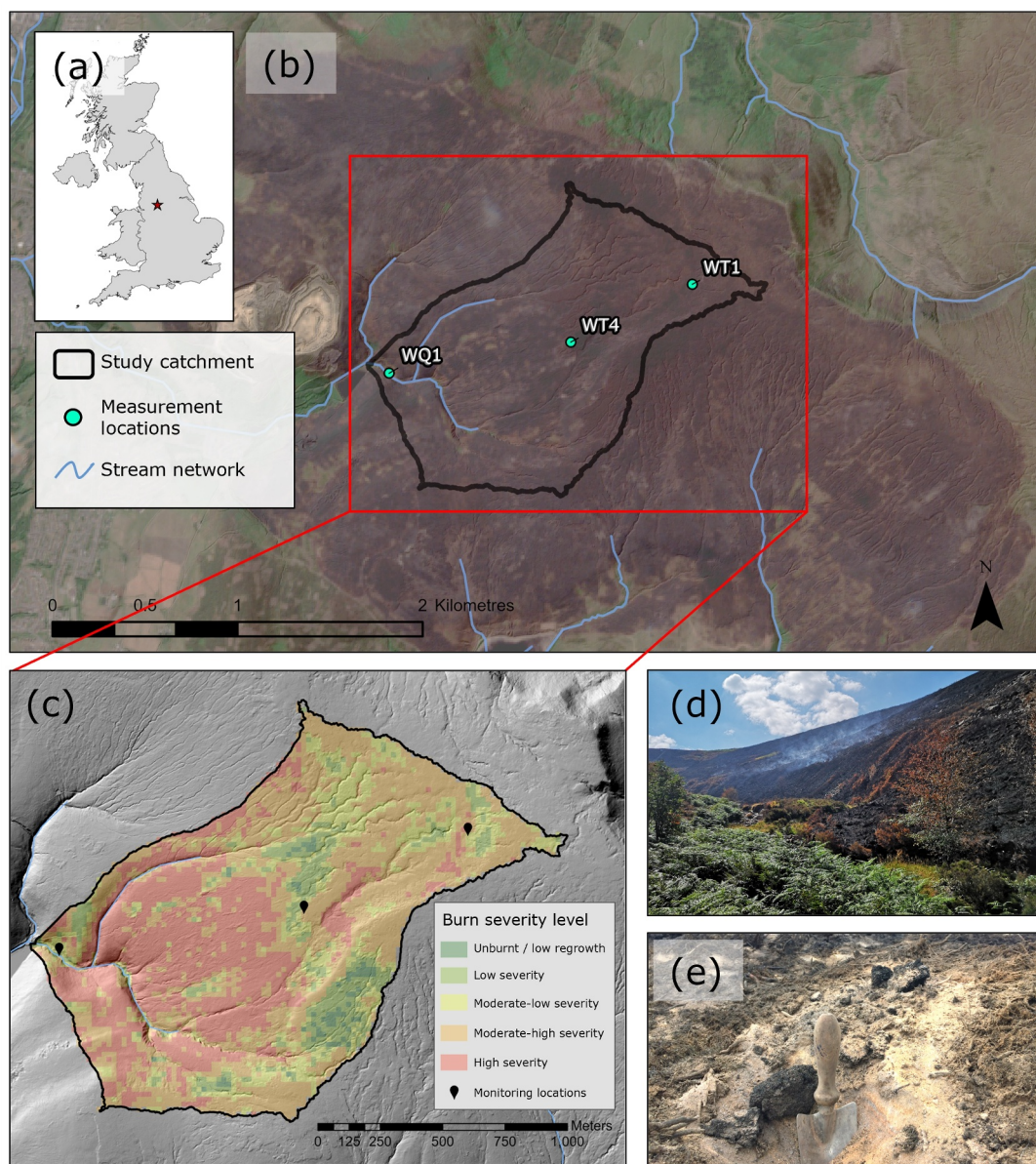


Figure 1. Overview of study area: (a) Approximate location of study catchment within the UK; (b) Landsat 8 aerial image (14 July 2018) of area after wildfire. Black line indicates the outline of the study catchment. WQ is the location of the stage instrument, WT1 and WT4 are locations where water table depths were measured; (c) Study catchment with difference Normalized Burn Ratio (dNBR) map overlay comparing Landsat images 24 June 2018 (pre-fire)–14 July 2018 (post-fire); (d) a view of the burnt catchment in the days following the wildfire taken at WQ1 monitoring location; and (e) an example of ash produced along the hillslope.

2.2.1. Precipitation and Continuous Stream-Flow Measurements

Continuous in-stream measurements were conducted at the catchment outlet (WQ in Figure 1b) between 12 July 2018 and 17 March 2019. The stream monitoring station was equipped with a Manta 2 multiprobe (Eureka, Texas, USA), connected to a CR100 data logger (Campbell Scientific, USA), which logged at 15-min intervals. The Manta 2 consists of the following sensing elements: (a) an electrical conductivity sensor; (b) a turbidity sensor, (λ 850 nm), (c) pH sensor, (d) an fDOM sensor for measuring humic-like fluorescence (λ_{ex} 325 nm, λ_{em} 470 nm), and (d) a thermistor for water temperature measurement. A pressure transducer—also connected to the CR100—was used to measure water level (PDCR-830, Druck Ltd, Leicestershire, UK).

The depth of water table below the surface (depth to water table; DWT) was measured at 15-min intervals through catchment-wide network dipwells (Figure 1b; Table S1 in Supporting Information S1), measured with a TD-Diver (Van Essen Instruments, Delft, the Netherlands). Dipwells WT1 and WT4 (Figure 1b) were taken into the analysis to be representative of varying water table depths in the headwaters (WT4) and the slope of hillslopes (WT1). These dipwells were selected because they had the most temporally complete data time series. Precipitation data at 15-min intervals were obtained from Environmental Agency station (#559586 Greenfield) located ~3 km away from the catchment.

2.2.2. Water Quality Measurements During Discrete Storm Events

Stream water samples were obtained during select discrete storm events with an autosampler (Teledyne ISCO 3700, Nebraska, USA) at WQ1 monitoring location (Figure 1b). The autosampler was programmed to collect samples every hour when storm events were anticipated, based on weather forecasts (1 day in advance) that predicted high chances of rainfall that would likely lead to significant runoff.

At the WQ stream monitoring site, the inlet tube was situated in the flow at the same depth as the Manta 2 sensing elements and a strainer was fitted to prevent blockage of the tubing. Samples collected for ICP-OES analysis were analyzed batch-wise at the Water Sciences Laboratory at the University of Birmingham. Before and after filtering, stream water samples from the storm events were stored in the refrigerator. Prior to analysis, Storms 1, 2, and 3 subsequently passed through a 0.7 μm filter and samples from Storms 4 and 5 passed through a 0.45 μm filter. These samples were analyzed for a range of elements using inductively coupled optical emission spectroscopy (hereafter referred to as ICP-OES): sodium (Na), magnesium (Mg), potassium (K), calcium (Ca), vanadium (V), magnesium (Mn), iron (Fe), nickel (Ni), cadmium (Cd), mercury (Hg), lead (Pb), boron (B), copper (Cu), zinc (Zn), aluminum (Al), phosphorus (P), sulfur (S), and arsenic (As).

The ICP-OES was calibrated before the analysis of each batch of sample runs using six different calibration standards in order of low to high concentrations; for these different dilutions of ICP multi-element standard solution was used. All calibration standards were prepared in ultrapure water. These calibration standards were followed by three laboratory blanks (ultrapure water), two quality control standards (MULTI-ELEMENT Standard solution for ICP-OES (supplied by CPAchem, Bulgaria), and a quality control containing 10 mg L⁻¹ of calcium, magnesium, sodium, and potassium), and three further laboratory blanks (ultrapure water). After every 20 samples, another blank (ultrapure water) and a quality control standard (MULTI-ELEMENT Standard solution for ICP) were analyzed to account for drift. Holmium, lutetium, indium, and scandium were used as internal standards in the ICP-OES analysis. Dissolved organic carbon (DOC) was determined using the Shimadzu TOC-TN Autoanalyzer analyser (Kyoto, Japan). Nitrate (NO_3^-), sulfate (SO_4^{2-}) and chloride (Cl) were measured with Dionex Ion chromatography (Thermo Fisher Scientific, California, USA) using three blanks.

Storm events with suitable data were used in the detailed analysis in the paper (selection criteria described in Section 2.3.2). Negative values of measured solutes were assumed to fall below the limit of detection and corrected to 0.001.

2.3. Data Processing and Analyses

2.3.1. Principal Component Analysis

A principal component analysis (PCA) was used as an exploratory tool to the measured solutes and other continuous variables to evaluate each variable's correlation to each other, and to reduce the number of parameters. The PCA was performed in R statistical software version 4.2.1 (R core team, 2022) using the *prcomp* function within the *stats* package, where data were zero-centered and scaled before performing the PCA using the *center* and *scale* arguments within the *prcomp* function. Based on the results of the PCA (described in Section 3.2), we selected nine variables for further analyses that were expected to be representative of different solute sources, disturbance impacts and/or transport behavior.

2.3.2. Storm Event Selection and Metrics

We captured a broad range of storm events during the 9 months post-fire. An in-depth analysis was performed for five discrete rainfall events (Figure 2), which captured the first two storm events post-fire, one storm in the autumn and two spring storm events including the highest discharge event of the year.

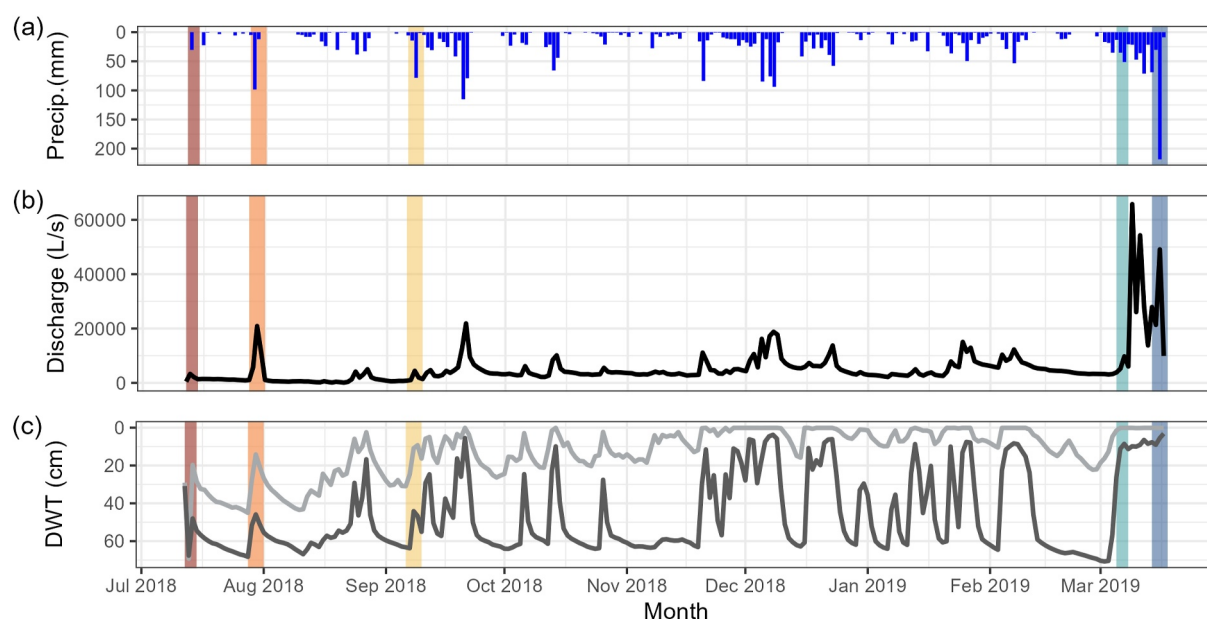


Figure 2. Daily totals of continuously measured variables from July 2018 until March 2019. The color bars running vertically in each graph denote individual storm events, for example, red = Storm 1 in July 2018 and dark blue = Storm 5 in March 2019; (a) Daily precipitation totals; (b) Daily discharge totals measured at WQ1; and (c) daily depth of water table (DWT) below the surface at middle catchment (WT4, light gray line) and upper catchment (WT1, dark gray line). The date of each storm event is as follows: Storm 1: 13–14 July 2018; Storm 2: 29–30 July 2018; Storm 3: 8–9 September 2018; Storm 4: 6 March 2019; Storm 5: 16–17 March 2019.

The area-velocity method was used to derive a discharge curve relationship derived from four in situ water level, velocity and stream channel area measurements—two of which were from the two largest storms of the year—and extrapolated by adjusting the Manning-Strickler equation (Chow et al., 1988), using parameters to represent the channel conditions at the outlet point. Missing data for short gaps (≤ 3 hr) in the measured time series were corrected by linear interpolation ($n \leq 3$).

Using the storm event data collected with the autosampler (described in Section 2.2.2), a storm event was defined as a clear rise in the flow with a first $\geq 1\%$ increase in discharge within 4 hr of the discharge peak after the onset of rainfall, and the end of the event was the first time there was $< 1\%$ decrease in discharge. Multipeak events were considered as one storm event in the analyses if the initial discharge peak value did not fall below 50% of the maximum discharge peak on the receding limb before increasing again. Similar storm event delineation criteria were used by Dupas et al. (2016) and Rozemeijer et al. (2010), with criteria values adapted to the stream flow of our study site.

We calculated antecedent conditions and within-storm metrics (Table 1), such as precipitation intensity and maximum depth of rainfall in any 30-min period (I30Max), to determine how flow dynamics and precipitation patterns impact storm event response solute behavior.

2.3.3. Calculating Event-Scale Hysteresis

Analysis of hysteretic behavior between measured water quality parameters and solute concentrations (C) and stream discharge (Q) was used to provide insights into source and transport mechanisms of solutes at the study site. We calculated the hysteresis index (HI; Lloyd et al., 2016) and flushing index (FI; Butturini et al., 2008) of each measured solute during each storm event. The HI describes the solute concentration change on the rising limbs and falling limbs of a storm event hydrograph. The FI describes a relative change in solute concentrations during the storm event: pre-event versus during event.

The HI ranges from -1 to 1 , where negative values indicate an anti-clockwise response and positive values indicates a clockwise response. We followed the interpretation of hysteresis by Lawler et al. (2006) where an anti-clockwise response occurs when the solute concentration is higher during the falling limb of the hydrograph. This indicates a distal solute source, delayed mobilization or distant delivery pathways to the outlet point. A clockwise

Table 1
Summary of Storm Event Characteristics and Antecedent Conditions During Each Storm Event

Category	Description	Storm 1	Storm 2	Storm 3	Storm 4	Storm 5
Rainfall	Total Rainfall during storm event (mm)	7.0	19.6	17.2	8.2	51.6
	Total 7-day antecedent rainfall (mm)	10.2	8.4	8.0	21.8	82.4
	Precipitation intensity (mm/h)	0.5	0.7	1.1	0.5	1.8
	Maximum 30-min intensity (I30 Max (mm/h))	8.0	6.8	14.8	4.0	6.4
Streamflow	Initial discharge (L/s)	16.31	13.51	10.60	37.36	134.78
	Maximum discharge (L/s)	268.51	359.20	317.9	80.5	976.44
Water table mid-catchment (WT4)	Initial depth to water table (m)	0.88	0.47	0.18	0.01	0.01
	Average depth to water table during event (m)	0.32	0.17	0.04	0.01	0.01
	Minimum depth to water table during event (m)	0.01	0.01	0.01	0.01	0.01
	Maximum depth to water table during event (m)	0.80	0.47	0.18	0.01	0.02
Water table upper catchment (WT1)	Initial depth to water table (m)	0.76	0.72	0.65	0.38	0.11
	Average depth to water table during event (m)	0.49	0.45	0.33	0.12	0.06
	Minimum depth to water table during event (m)	0.17	0.17	0.01	0.10	0.02
	Maximum depth to water table during event (m)	0.76	0.72	0.65	0.38	0.11

response occurs when solute concentration is higher on the rising limb of the hydrograph, which can indicate that a solute is sourced from a readily available source or transported along relatively short pathways.

The HI is calculated using the normalized values of both solute concentration (C) and discharge (Q), at the k th percentile of the flow. Normalized C ($C_{i \text{ norm}}$) was linearly interpolated between adjacent measurements at every 1% intervals of discharge ($Q_{i \text{ norm}}$). The following Equations 1 and 2 were used to calculate $C_{i \text{ norm}}$ and $Q_{i \text{ norm}}$:

$$C_{i \text{ norm}} = \frac{C_i - C_{\min}}{C_{\max} - C_{\min}} \quad (1)$$

$$Q_{i \text{ norm}} = \frac{Q_i - Q_{\min}}{Q_{\max} - Q_{\min}} \quad (2)$$

Where C_i and Q_i are the discharge and solute at timestep i in the storm event. The subscripts min and max represent the minimum and maximum, respectively, of Q or C . The percentiles of discharge (Q_i) are calculated as follows:

$$Q_i = k(Q_{\max} - Q_{\min}) + Q_{\min} \quad (3)$$

Where Q_{\max} is the peak discharge, Q_{\min} is the discharge at the start of the event and k is the point along the loop where the calculation is being made; in this case the index was calculated at every 1% (thus $k = 0.01, 0.02, 0.03, \dots, 0.99, 1.0$). The HI is then calculated as:

$$HI_{Q_i} = CRL_{Q_i} - CFL_{Q_i} \quad (4)$$

Where HI_{Q_i} is the HI at the i th percentile of discharge (Q), CFL_{Q_i} represents concentration values on the rising limb at a certain percentile i of Q ; and CRL_{Q_i} represents the concentration values on the falling limb at a certain percentile i of Q . The mean HI was calculated from each individual HI_{Q_i} value.

The flushing index (FI) also ranges from -1 to 1 , where negative values indicate a dilution response: solute concentrations are diluted by storm water. Positive values indicate a flushing/concentration response, demonstrating that solute concentrations are higher or enriched with increasing flow (Heathwaite & Bierzoza, 2021; Liu et al., 2021). FI was calculated using the following equation:

$$FI = C_{Q_{peakNorm}} - C_{initialNorm} \quad (5)$$

Where $C_{Q_{peakNorm}}$ and $C_{initialNorm}$ are the normalized solute concentrations at the peak discharge (largest peak discharge in the case of a multi-peak event) and the solute concentration at the beginning of the storm, respectively.

C-Q relationships were established to further describe solute dynamics within storm events. C-Q relationships contribute to identifying temporal patterns in data by comparing solute concentrations on the rising limb and the falling limb of a hydrograph for a given storm event to infer processes that control solute source zones, contributing flow sources and transport pathways in a catchment during storm events (Blaen et al., 2017; Liu et al., 2021; Lloyd et al., 2016; Zuecco et al., 2016). All data are normalized between 0 (minimum measured value for the event) and 1 (maximum measured value for the event) for better visualization of the hysteretic relationship. C-Q graphs were visually inspected and classified in terms of their direction into clockwise, anti-clockwise and complex response patterns (e.g., figure of eight-shaped; described in Section 3.3). All calculations and analyses were completed in R Statistical software version 4.2.1 (R core team, 2022).

3. Results

3.1. Characterization of Hydrological Response

Hydrological monitoring of the catchment began 13 days after the fire. During the 9 month monitoring period, progressive rainfall events gradually rewetted the catchment. The five storm events we selected for detailed analysis occurred along this trajectory (Figure 2), leading to differences in antecedent conditions prior to the storm events (Table 1). The first two post-fire storm events occurred in the summer after a prolonged period with little rainfall following the intense drought period, with deep water table levels (Figure 2b; Table 1). During these two storm events, the water table and stream flow responded quickly following precipitation events (Figure 2a). The average DWT in Storms 1 and 2 changed from 0.49 to 0.45 m at WT1 and from 0.32 to 0.17 m at WT4, indicating shallower water tables relative to the ground surface. Storm 2 was a large, multi-peak event, with the highest maximum discharge of the summer and autumn storms (359.20 L/s). During this storm event, the DWT increased to a maximum DWT of 0.72 m at WT1 and 0.47 m at WT4—similar to the maximum DWT at WT1 of Storm 1.

There was little precipitation in the 7 days prior to Storm 3 in the autumn (8.0 mm; Table 1) and the stream flow response showed a relatively small discharge peak. The water table, however, was closer to the surface at mid-catchment (max. DWT 0.18 m; Table 1) compared to Storms 1 and 2. The depth to water table in the mid-catchment (WT4; Figure 2b) remained slightly elevated in the autumn after Storm 3 (Figure 2) whereas in the upper catchment (WT1) water table resurgence, likely due to precipitation, was more common throughout the measurement series until March 2019.

In the time between September 2018 and March 2019 (Storm 3 and Storm 4), there were relatively few high discharge events (Figure 2a). The water table remained shallow for longer periods of time after storm events in the winter, in line with gradual catchment rewetting. In the springtime, antecedent precipitation (21.8 mm; Table 1) preceding Storm 4 was high. During the storm, the DWT shallow relative to the surface following the event, likely as a result of continued rainfall in the spring. Storm 5, a multi-peak event, was the largest storm event in the series (max. discharge 976.44 L/s), and also had the highest total precipitation during the storm event (51.6 mm) and highest average precipitation intensity (1.8 mm/hr).

3.2. Stormflow Stream Water Chemistry

3.2.1. Principal Component Analysis

The PCA analysis for all of the measured solutes and variables in our study produced four components with eigen values >1. Figure 3 shows the first two components, which together explain 66.5% of the variance. The solutes clustered in component space around different storm events (Figure 3). The first ordination axis separated the summer storm (left: storm 1) from the spring storms (right: storm 4 and 5), and was characterized by negative loadings of nutrients and base cations to the left, and positive loadings of many metals and turbidity to the right. The second ordination axis separated the two autumn Storm 3 (top) and Storm 2 (bottom), with positive loadings of Mn and Al and negative loading of pH.

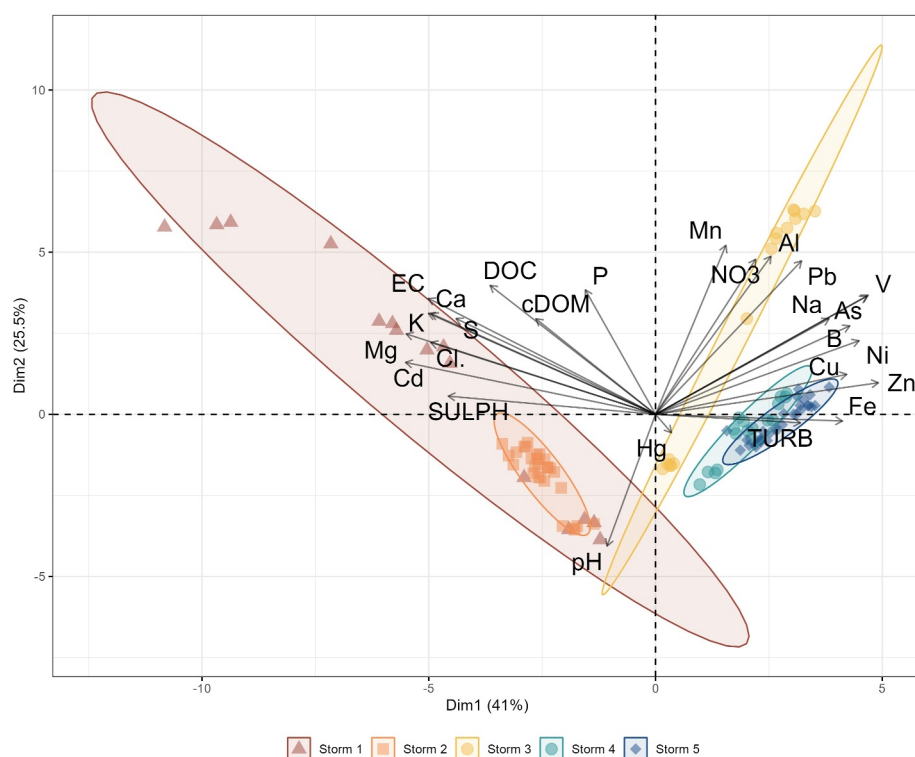


Figure 3. Principal component analysis (PCA) of all measured water quality parameter measured at the stream outlet (WQ1). Different colored dots with the same individual symbol represent the different storm events (i.e., red triangle = Storm 1, yellow circle = Storm 3). The ellipses are color-coordinated with their respective storm events, which represent the 95% confidence interval around the centroid (mean) position for each storm event within the PCA space.

Variables negatively loaded on PC1 and positively loaded on PC2 (i.e., in the upper left quadrant) are most likely associated with post-fire burnt materials—such as charcoal and ashes—and drought conditions of the catchment. Solutes positively loaded on PC1 and PC2 (upper right corner) are primarily associated with the spring storm events that occur during the wetter catchment conditions shown in Figure 2. PC2 is influenced strongly by pH, potentially indicating different water source zone in the catchment that are more acidic dominated. Given the distribution of these variables in the PCA and clustering around different storm events, we selected solutes that we consider to be representative of different source zones and solutes that may be representative of wildfire ashes or drought impact in the catchment (Bodí et al., 2014; Stirling et al., 2020): turbidity (TURB), dissolved organic carbon (DOC), sulfate (SO_4^{2-} ; SULPH), calcium (Ca), aluminum (Al), lead (Pb), sodium (Na), copper (Cu), and zinc (Zn).

3.2.2. Stormflow Solute Concentrations

Highest concentrations of DOC, SO_4^{2-} and Ca occurred in the first two storms immediately following the wildfire (~0–3 months post-fire) and were much lower in the autumn and spring (~3–9 months post-fire) (Figure 4; Table S1 in Supporting Information S1). While the highest pH value amongst the storm events in our study occurred in Storm 1 (6.5), the median value was the highest (4.8) in Storm 4 in comparison to the other storm events. Na had lower concentrations in the Storms 1 and 2 immediately following the fire (712.5 and 830.3 ppb, respectively) and its highest concentration in autumn (Storm 3; 6998.2 ppb).

Most metals (Al, Pb, Cu, and Zn) showed a small increase in concentration immediately after the fire (Figure 4). But in general, metal concentrations were higher in autumn and into the spring storms (Figure 4; Table S2 in Supporting Information S1). Notably, Na, Pb, and Al had their highest concentrations in Storm 3 (6996.2, 3.4, and 1014.9 ppb, respectively), and their concentrations were also elevated in the spring storms. Cu and Zn had their highest concentrations in Storm 4 (4.3 and 291.72 ppb, respectively) and remained elevated in Storm 5 compared to the earlier storm events.

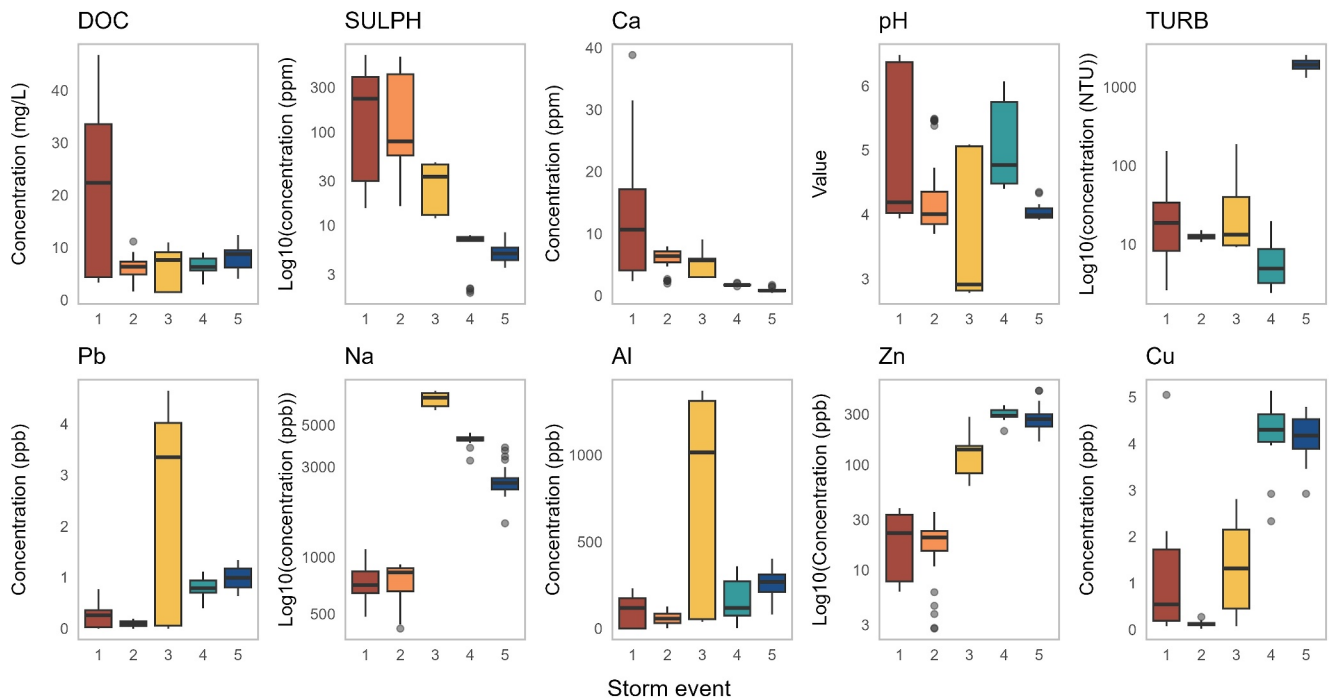


Figure 4. Concentrations of each variable and solute during the storm events. The different colors represent the different storm events, with warmer colors for summer and autumn (Storm 1–3), and cooler colors for the spring storm events (Storm 4–5). The black horizontal line in the middle of each box plot represents the median value. Note that y-axis of SULPH (sulfate), TURB (turbidity), Na and Zn are plotted on a log scale to improve readability of extreme values, and note the different values on the y-axis for each variable and solute.

Turbidity in Storms 1–4 was low (18.2–4.7 NTU) in comparison to Storm 5, the final spring storm event. Observations from the field following this storm event noted large channel erosion and channel bank failure near the outlet, and therefore likely contributing additional sediment to the stream.

3.3. Solute Behavior Patterns

A range of hysteresis indices (HI) and flushing indices (FI) were observed for the five storms (Table S3 in Supporting Information S1). The overall dominant HI response was anti-clockwise (60% of all measured variables) where solute concentration peaks after the discharge peak. Clockwise hysteresis, where solute concentration peaks before the discharge peak, was less frequently observed. Flushing index (FI) values were generally positive, indicating a flushing for most solutes (82%), meaning that the solute concentration often increased as discharge increased. HI and FI for the nine selected solutes are reported in-text, and all measured variables are reported in Table S3 in Supporting Information S1.

The HI of most nutrients and base cations had an anticlockwise HI response (mean $-0.25 \pm 0.28 SE$) and flushing FI response (mean $0.64 \pm 0.49 SE$) (Storms 1, 2, and 3; DOC, Na, Ca, SO_4^{2-}), suggesting rapid mobilization in these storm events following the wildfire. The response shifted toward a clockwise HI response (mean HI $0.09 \pm 0.29 SE$) and a dilution FI response (mean $-0.12 \pm 0.59 SE$) in the spring storms. Most metals often had an anticlockwise response in all storm events, indicating a predominance for delayed mobilization, except for the last storm event (Storm 5). The shift away from anti-clockwise HI response in the final storm event (Storm 5) may be due to the multi-peak nature of the storm event and the HI not being able to capture the complex nature of the solute behavior.

3.3.1. C-Q Response Patterns

The dominant observed C-Q response patterns, illustrated in Figure 5a, provide more insight on temporal behavior within each storm event. Anti-clockwise C-Q was the most common response in all storm events, especially in the storms within the first 3 months following the wildfire (~0–3 months; Storms 1, 2 and 3), in line

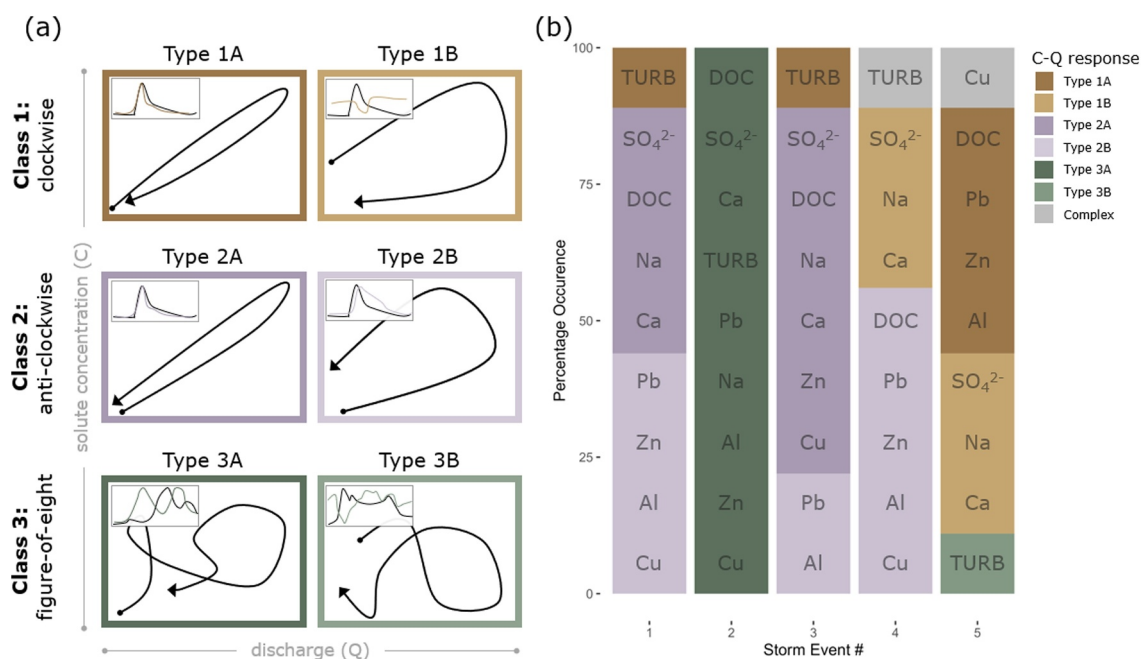


Figure 5. (a) Schematic overview of classes of observed C-Q patterns in the study catchment, where Class 1 is clockwise C-Q response, Class 2 is anti-clockwise C-Q response and Class 3 is figure-of-eight or complex C-Q response. The different types—for example, Type 1A versus Type 2A—represent further the shape of the C-Q response pattern; (b) percentage occurrence of each solute C-Q behavior for each respective storm. Solutes are shown in gray text, grouped into their respective C-Q response per storm, on top of the bar graph.

with the HI index. In Storms 1 and 3, turbidity showed a clockwise C-Q response (Type 1A; Figure 5b), which is indicative for rapid transport.

Metals (Pb, Zn, Al, Cu) displayed anti-clockwise C-Q behavior (Types 2A and 2B; Figure 5b) in most storms, where solute concentrations peaked after the discharge peak. In Storm 1, response Type 2B—a large C-Q loop—dominated. In the third month after the wildfire (Storm 3), Cu and Zn displayed Type 2A response, which is indicative of a quicker increase of the solute concentration relative to discharge, whereas Pb and Al still displayed response Type 2B.

All solutes display complex C-Q behavior—Type 3A—in Storm 2 (Figure 5b). This is likely owing to the timing of precipitation at the beginning of the storm event (Figure 2a). Most nutrients and base cations (SO_4^{2-} , Na and Ca) shift to clockwise C-Q responses (Figure 5b) in the springtime March storm events. In the last storm event of the time series (Storm 5, ca. 9 months after fire), SO_4^{2-} , Na and Ca displayed Type 1B, which is consistent behavior as the previous storm. Here several parameters exhibited clockwise response, including most metals (Figure 5b). Different from the C-Q responses of the measured solutes, turbidity displayed a figure-of-8 response (Type 3B) in Storm 5.

4. Discussion

4.1. Hydrological and Biogeochemical Wildfire Response

The highest median concentrations of Ca, DOC and SO_4^{2-} (and many other base cations and nutrients; Table S2 in Supporting Information S1) occurred in the first two storm events post-fire in the summer, and were generally lower in the spring storms. The slightly higher availability of these solutes in the immediate post-wildfire storms is presumably a coupled wildfire ash impact and drought response. Average concentrations of DOC in Storm 1 in the stream flow (22.16 mg/L) are similar to those observed in an un-burnt catchment in the region (~20–30 mg/L) (Rothwell, Evans, & Allott, 2007; Rothwell, Evans, Daniels, & Allott, 2007). However we observed slightly higher maximum DOC concentrations (46.74 mg/L) in Storm 1 compared to maximum values observed by Rothwell, Evans, Daniels, and Allott (2007) and Rothwell, Evans, and Allott (2007) (35.9 mg/L). In the remaining storm events from our study, though, average DOC concentrations in the stormflow were

comparatively much lower ($\sim 6\text{--}8$ mg/L). Average SO_4^{2-} concentrations in Storms 1 and 2 was ~ 250 ppm, much higher than values observed in a comparable un-burnt catchment within the region where average sulfate concentrations ranged from $\sim 50\text{--}80$ $\mu\text{eq/L}$ (from April to November) (Daniels, Agnew, et al., 2008; Daniels, Evans, et al., 2008). Sulfate concentrations are much lower in the subsequent storm events (Figure 4). SO_4^{2-} is often formed during periods of drought due to the oxidate of sulfur stored in the peat as a result of water table drawdown (Clark et al., 2005; Juckers & Watmough, 2014). Elevated concentrations of SO_4^{2-} and DOC in the first storm event are therefore most likely a drought response, attributed to mobilization of pre-existing old material by storm water influx following the extended dry period (Tiwari et al., 2022). Elevated DOC concentrations reported in our study are relatively consistent with a burnt peatland in the Canadian boreal region, where DOC yields were slightly lower in the spring and elevated in the summer season following wildfire (Burd et al., 2018); however, DOC hysteresis patterns shown in Burd et al. (2018) were dissimilar from our study. This suggests that differing landscape characteristics may influence transport patterns within burnt catchments, thus making it difficult to fully substantiate wildfire impacts on DOC behavior and yield between the two regions.

The lower concentrations of many base cations and nutrients in the autumn and spring storm events indicates catchment recovery following the disturbances. Given the large amount of ash produced throughout the site, especially in high burn severity areas and on the steeper mid-slopes (Figure 1e), we believe that ash-related elements could have been exhausted from the catchment, which could be the ash leachate that exhausted and represents a nutrient flux to soils (Swindle et al., 2021) and not necessarily the physical ash exhaustion itself. Additionally, the nutrients from the ash could fertilise vegetation during regrowth (Bodí et al., 2014). Therefore, while ash or its leachates may be transported quickly in the fluvial network during the first post-wildfire storms, the amount of ash may be limited or become diluted in the immediate months following the fire (Marcotte et al., 2022; Sánchez-García et al., 2023; Santín et al., 2015), even if large swaths of ash remain on the surface and become covered by vegetation regrowth, as observed during a field visit 3 years following the wildfire event. While we acknowledge that the decrease in total concentrations of solutes between Storms 3 and 4 may partly be an artefact of the change of filter paper size during sample preparation, differential behaviour among solutes retains its indicative value and their dynamics throughout the storm events are well-captured within our study.

The C-Q response (Type 2A; Figure 5) of the drought- and fire-associated elements indicate that transport of these solutes occurred rapidly. Coupled with deeper water table and low antecedent wetness conditions prior to the early storm events, solutes—such as DOC, Ca and Na—are likely sourced from areas close to the stream, perhaps due to disconnection from the larger stream network, which can result in shorter transit time (van Meerveld et al., 2019). Additionally, increased hydrophobicity post-wildfire (Wu et al., 2020) may have contributed to enhanced surface runoff (Shakesby & Doerr, 2006) and associated rapid transport of burnt materials left on the soil surface. Together, the short transit times coupled with dry conditions enhancing surface hydrophobicity (Evans et al., 1999) may have hindered the dominance of subsurface transport pathways—as well as solute source zones beyond the stream corridor—in the catchment in the ~ 3 months following the wildfire. While the focus of this study is primarily hydrology-focused, it is worth noting that both ash and eroded peat at our study site can be dispersed by wind even outside the fire perimeter (Bodí et al., 2014), thus increasing spatial complexity of potential wildfire impacts on water quality.

Nutrients and base cations displayed a shift to dilution FI and C-Q patterns in the spring storms (Storms 4 and 5). The behaviour may be influenced by wetter antecedent conditions at the time of the two storms. For example, while Storm 4 was small in terms of discharge, the higher antecedent wetness at the time of the storm event can quickly mobilise solutes and sediment but cause a swift decline in concentration during the storm event (Hamshaw et al., 2018). Such flushing behaviour may also indicate that the solutes are transported from the deeper subsurface layers, rather than within the fast flow. Studies have noted that ground water sourced and bedrock derived solutes, such as Ca, often exhibit this behaviour as their concentration decreases with increasing discharge (Heathwaite & Bieroza, 2021; Knapp et al., 2022). This shift may then indicated a change from surface transport of readily available burnt materials, such as ash, to an exhaustion of said materials in the months after the initial post-fire storm events. However, in blanket peatland systems such as our study site, it is probable that nutrients and base cations exhibiting dilution FI and anti-clockwise HI (Figure 5) could be transported subsurface through the pipe network, given that they are transported on the rescinding discharge limb (Daniels, Agnew, et al., 2008; Daniels, Evans, et al., 2008), and surface peat layers are generally low in Ca. Given the underlying strata in our catchment contains CaCO_3 (Wolverson-Cope, 1976), the stream will come into contact with the carbonate rich

waters where the stream cuts through the peat profile or comes into the exposed bedrock near the outlet, thus potentially contributing to elevated Ca concentrations (Worrall et al., 2003).

4.2. Metal Activation Influenced by Drought Recovery

Peak median concentrations of Na, Pb and Al occurred early autumn, and high median concentrations of Cu and Zn occurred in the spring storm events, coinciding with the timing of catchment rewetting. We did not observe highly elevated metal concentrations in the stream flow immediately after the wildfire (Figure 4). While the wildfire may have enhanced metal release from the peat, this particular wildfire was likely not the main factor in enhancing dissolved metal transport from source zones to the stream outlet in the catchment. Rather, the reconnection of headwater source zones with the stream network seemed key for solute loading and transport downstream (Freeman et al., 2007).

The acute peak of metals after the wildfire in the first storm event may be because wildfire ash can be enriched with metals that may be redistributed into the landscape or fluvial system (Bodí et al., 2014; Pereira et al., 2012; Sánchez-García et al., 2023), however these metal peaks were not as high compared to subsequent storm events. Average streamflow Pb values from the storm events in our study (0.26–2.30 ppb) are comparatively lower than Pb values reported in the area from an unburnt catchment (average 4.45–9.46 ppb; (Rothwell, Evans, Daniels, & Allott, 2007)). Average Cu concentrations during our study period were also comparatively lower to values from the unburnt catchment reported in Rothwell, Evans, Daniels, and Allott (2007) and Rothwell, Evans, and Allott (2007) (0.12–4.15 ppb vs. 4.01–7.92 ppb, respectively). Conversely, average Zn concentrations during our study were initially low in Storms 1 and 2 compared to values reported in Rothwell, Evans, Daniels, and Allott (2007) and Rothwell, Evans, and Allott (2007), yet were much higher in Storms 3–5. On average, Zn concentrations during the final three storm events ranged from 139.17–303 ppb, whereas average Zn concentrations reported in the unburnt catchment ranged from 50.5–71.8 ppb (Rothwell, Evans, & Allott, 2007; Rothwell, Evans, Daniels, & Allott, 2007). Sánchez-García et al. (2023) report mean concentrations of ash samples collected from the 2018 Stalybridge fire (from the same burnt area as this study), showing high dissolved concentrations of Al, Pb, and Zn in the ash compared to other non-metal parameters. In addition to a potential ash impact, post-drought mobilization of metals during re-wetting has been observed in boreal peatlands (Szkokan-Emilson et al., 2013) and other peatland systems (cf., Stirling et al., 2020).

Some metals from our study (Na, Pb, Al) had their highest median concentration in the autumn storm (Storm 3). Because the headwaters were only consistently connected later in the season as the catchment began recovering from the drought, this likely influenced the activation of many metal source zones. A significant proportion of the metals that may have been released during the wildfire are likely stored and bound to the peat in the headwaters of the catchment, or potentially stored in peat particles behind re-growing vegetation acting as sediment traps and thus not being easily entrained and transported (Shuttleworth et al., 2017). This could account for the low observed values of many metals in the streamflow at our study site.

The delayed mobilization of metals is, for the most part, reflected in the C-Q responses. Metals (Pb, Zn, Al, Cu) mainly exhibited anti-clockwise HI and Type 2B (anti-clockwise) C-Q patterns, suggesting a predominately within-peatsource further upslope or in the headwaters of the study catchment. The delayed transport may also indicate occurrence of saturation excess overland flow, commonly observed in blanket peatlands where flow can persist even after rainfall due to slower drainage from the hillslopes (Holden & Burt, 2003).

While DOC did have its highest average concentration in the first post-wildfire storm, its C-Q behavior shifts to align with metals (Type 2B) in the spring storms (Storms 4 and 5). This suggests that metal transport can be related to DOC export through complexed metals (Lawlor & Tipping, 2003; Rothwell, Evans, & Allott, 2007; Rothwell, Evans, Daniels, & Allott, 2007) as the spring season progresses. DOC export is perhaps also linked to seasonality, with higher concentrations occurring in the summer owing to higher temperature (Clark et al., 2005), and would indicate that DOC and metals share a similar source zone.

It is worthwhile to note that multivalent cations Al and Pb exhibited anti-clockwise C-Q response (Type 2B) in the autumn storm (Storm 3), indicating slower transport. Whereas Cu and Zn deviated and showed rapid anti-clockwise C-Q response (Type 2A), which could indicate rapid overlandflow, flushing through the acrotelm (Rothwell, Evans, & Allott, 2007; Rothwell, Evans, Daniels, & Allott, 2007) or transport via pipeflow. Given the patchy presence of the acrotelm in our headwaters, overland flow or flow through pipes seems more probable. The

similar C-Q response of Al and Pb points that they are sourced from similar source areas that are likely more in the headwaters—hence their delayed and slow transport to the stream outlet. The varying responses of metals may also be due to heterogeneity in solute sources, for example, the vertical versus lateral distribution within the catchment and peat profile which can be heterogeneously activated under dry versus wet conditions (Knapp et al., 2022). In addition to heterogeneous solute source zones, it is likely that solutes which are more efficiently mobilized, such as monovalent cations, have higher concentration in the post-wildfire storms and the metals bound to the peat, such as multivalent cations, are mobilized later in the monitoring period. Furthermore, concentrations of solutes in the fluvial system due to wildfire impacts is driven not only by hydrological extreme events (e.g., flooding) but also through biogeochemical alterations in the peat soil profile. Adsorption to soil and organic matter of metals, and its desorption, is highly site-specific and is affected by several aspects such as the nature of bonding strength, pH of the peat matrix, redox potential and the background concentration of the metals (e.g., Brown et al., 2000; Twardowska & Kyzioł, 2003). However, a detailed investigation into geochemical mechanisms of metal detachment and mobility was not within the scope of this study. Further research on mobility dynamics as influenced by these variables can help to disentangle hydrological and geochemical controls on mobility of metal and other pollutants under changing climate extremes.

In Storm 5—the last storm of our set in the spring—DOC, Pb, Zn, and Al exhibited rapid clockwise transport (Type 1A), suggesting that their mobilization and rapid transport may be influenced by saturation excess overland flow—a dominant runoff pathway in blanket peatlands (Holden & Burt, 2003)—as precipitation intensity is noted as key driver of runoff responses in large magnitude storms in this region (Edokpa et al., 2022). Given that the hillslopes were likely well-connected to the stream network, it is possible that metal storages within the peat are more efficiently hydrologically activated, thus readily available for mobilization and transport. For example, in the springtime the soil profile was likely vertically and laterally hydrologically connected with the fluvial network, thus allowing metals to flush through the saturated acrotelm during storm events associated with high flows and higher water tables (Holden, 2006; Rothwell, Evans, & Allott, 2007; Rothwell, Evans, Daniels, & Allott, 2007).

4.3. Wider Relevance

Temperate peatlands are facing an increase of severe drought and wildfire conditions due to climate change (Albertson et al., 2010). Despite this, there is still a significant knowledge gap regarding the influence of such disturbances on the fate of hydrologic functioning and water quality in these regions. We postulate that wildfires in this catchment may not currently enhance the risk of metal transport immediately following disturbances as much as originally suggested by other studies in this region, given that the source zones of most metals were not as effectively hydrologically connected to the fluvial system within the window of disturbance. It is worth noting that metals are most likely also bound to the organic matter in our catchment (Shuttleworth et al., 2014). Yet despite the high concentration of potentially toxic metals stored in the peat profiles noted in this region, their direct availability may be limited until repeated disturbances cause additional degradation in the future that contribute to the increased availability of metals. Over time, the metals stored in both the ash and the metal-rich peat particles (Rothwell et al., 2005) may have a disproportionate influence on water quality in the receiving reservoir rather than directly on stream water chemistry. Further research on within-catchment source and mobility of metals is needed for improved risk assessment.

The occurrence of clockwise, anticlockwise and complex hysteresis patterns occurring at different times within the same catchment highlights the influence of event characterization and catchment conditions such as burn severity and topography—rather than solely stream discharge—on solute activation and transport dynamics. However, given the short time span of our data set and lack of high resolution baseline data, it is challenging to fully disentangle response variability due to post-disturbance adaptation from what could be common seasonality patterns (Clark et al., 2008), highlighting that post-wildfire hydrological research will often be naturally hampered by lack of pre-wildfire data (i.e., Basso et al., 2021; Robinne et al., 2021). Furthermore, hydrologic processes within blanket peatlands are not straightforward, as hillslope runoff pathways are highly spatially and temporally heterogeneous (i.e., Holden & Burt, 2003). We therefore recommend future studies of high resolution solute dynamics to capture post-wildfire storm events over multiple seasons (i.e., Nunes et al., 2020), and ideally in a pre-fire context, in order to have a better picture of response patterns dependent on season or intrastorm rainfall structure and runoff patterns.

Studies indicate that water table drawdown exacerbates the risk of ignition and fire severity in peatlands (Waddington et al., 2015; Wilkinson et al., 2020), consequently, intensifying wildfire activity that accelerates peat degradation and the likelihood of subsequent wildfires (Kettridge et al., 2015). For example, wildfires during wetter periods and higher hydrological catchment connectivity may not be as severe due to limited burn severity of saturated peat. Conversely, wildfires occurring during dryer periods and low hydrologic catchment connectivity may have limited impacts, as mobilised elements can be recaptured or impeded by recovering vegetation and soil (Caon et al., 2014). The growing risk of climate change-induced drought, wildfire events and increasing incidence of large summer storms leaves temperate peatlands vulnerable to further degradation such as altered hydrologic processes and enhanced erosion (Evans et al., 1999), and subsequent negative impacts on water quality (McCarter et al., 2023; Wilkinson et al., 2023). Future studies would be strengthened by quantifying areas of concern within the catchment that store different pools of nutrients and metals to better identify high-risk zones, for example, through tracer studies (e.g., Tetzlaff et al., 2015), and how solutes may be entrained in the fluvial system. Monitoring receiving bodies of water will also advance our understanding of the longevity the elements in the reservoir, and the potential impacts on ecosystems and human health.

5. Conclusion

We have found a wide range of solute responses following severe wildfire and drought conditions in a temperate peatland dominated catchment. Concentration-discharge relationships were analyzed to infer solute source zones and transport pathways within the disturbed catchment. Immediately after the wildfire, nutrient and base cation concentrations had their highest average concentrations, gradually decreasing over the subsequent months. In contrast, metal concentrations showed an increasing trend during autumn and into the spring storms, coinciding with catchment re-wetting. These patterns suggest the rapid mobilization and flushing of nutrients and base cations after the wildfire and drought, followed by dilution behaviors in the spring storms. Notably, metals consistently exhibited delayed mobilization, peaking after the discharge peak, indicating sources within the peat or distal headwaters rather than being predominately sourced from ash or near the downstream reaches of the stream (i.e., proximal sources). Our findings highlight the importance of seasonal re-wetting with rejuvenated hydrological connectivity for the detachment, mobilization and transport of solutes in the study catchment following extreme drought and wildfire. Findings from our study contribute to a critical understanding of the future of water quality risks in temperate peatland catchments subject to extreme disturbances such as drought and wildfire.

Conflict of Interest

The authors declare no conflicts of interest relevant to this study.

Data Availability Statement

Data used in the analyses for this manuscript are publicly available at the following <https://doi.org/10.5281/zenodo.11235836>.

References

- Albertson, K., Ayles, J., Cavan, G., & McMorrow, J. (2010). Climate change and the future occurrence of moorland wildfires in the Peak District of the UK. *Climate Research*, 45(1), 105–118. <https://doi.org/10.3354/cr00926>
- Basso, M., Mateus, M., Ramos, T. B., & Vieira, D. C. S. (2021). Potential post-fire impacts on a water supply reservoir: An integrated watershed-reservoir approach. *Frontiers in Environmental Science*, 9. <https://doi.org/10.3389/fenvs.2021.684703>
- Bindler, R. (2006). Mired in the past—Looking to the future: Geochemistry of peat and the analysis of past environmental changes. *Global and Planetary Change*, 53(4), 209–221. <https://doi.org/10.1016/j.gloplacha.2006.03.004>
- Bladon, K. D., Emelko, M. B., Silins, U., & Stone, M. (2014). Wildfire and the future of water supply. *Environmental Science & Technology*, 48(16), 8936–8943. <https://doi.org/10.1021/es500130g>
- Blaen, P. J., Khamis, K., Lloyd, C., Comer-Warner, S., Ciocca, F., Thomas, R. M., et al. (2017). High-frequency monitoring of catchment nutrient exports reveals highly variable storm event responses and dynamic source zone activation. *Journal of Geophysical Research: Biogeosciences*, 122(9), 2265–2281. <https://doi.org/10.1002/2017JG003904>
- Bodí, M. B., Martín, D. A., Balfour, V. N., Santín, C., Doerr, S. H., Pereira, P., et al. (2014). Wildland fire ash: Production, composition and eco-hydro-geomorphic effects. *Earth-Science Reviews*, 130, 103–127. <https://doi.org/10.1016/j.earscirev.2013.12.007>
- Bower, M. M. (1961). The distribution of erosion in blanket peat bogs in the Pennines. *Transactions and Papers*, 29, 17–30. <https://doi.org/10.2307/621241>
- Brown, P. A., Gill, S. A., & Allen, S. J. (2000). Metal removal from wastewater using peat. *Water Research*, 34(16), 3907–3916. [https://doi.org/10.1016/S0043-1354\(00\)00152-4](https://doi.org/10.1016/S0043-1354(00)00152-4)

Acknowledgments

This project has received funding from the European Union's Horizon 2020 research and innovation programme under the Marie Skłodowska-Curie Grant 860787. A.L. Marcotte is grateful to Luc Steinbuch for coding assistance. The authors thank the three anonymous reviewers for their time and suggestions that helped to improve the manuscript.

- Burd, K., Tank, S. E., Dion, N., Quinton, W. L., Spence, C., Tanentzap, A. J., & Olefeldt, D. (2018). Seasonal shifts in export of DOC and nutrients from burned and unburned peatland-rich catchments, Northwest Territories, Canada. *Hydrology and Earth System Sciences*, 22(8), 4455–4472. <https://doi.org/10.5194/hess-22-4455-2018>
- Butturini, A., Alvarez, M., Bernal, S., Vazquez, E., & Sabater, F. (2008). Diversity and temporal sequences of forms of DOC and NO₃-discharge responses in an intermittent stream: Predictable or random succession? *Journal of Geophysical Research*, 113(G3), G03016. <https://doi.org/10.1029/2008JG000721>
- Caon, L., Vallejo, V. R., Ritsema, C. J., & Geissen, V. (2014). Effects of wildfire on soil nutrients in Mediterranean ecosystems. *Earth-Science Reviews*, 139, 47–58. <https://doi.org/10.1016/j.earscirev.2014.09.001>
- Chafer, C. J., Santín, C., & Doerr, S. H. (2016). Modelling and quantifying the spatial distribution of post-wildfire ash loads. *International Journal of Wildland Fire*, 25(2), 249–255. <https://doi.org/10.1071/WF15074>
- Chow, V. T., Maidment, D. R., & Mays, L. W. (1988). *Applied hydrology*. McGraw-Hill. Retrieved from <http://catdir.loc.gov/catdir/toc/mh021/87016860.html>
- Clark, J. M., Chapman, P. J., Adamson, J. K., & Lane, S. N. (2005). Influence of drought-induced acidification on the mobility of dissolved organic carbon in peat soils. *Global Change Biology*, 11(5), 791–809. <https://doi.org/10.1111/j.1365-2486.2005.00937.x>
- Clark, J. M., Lane, S. N., Chapman, P. J., & Adamson, J. K. (2008). Link between DOC in near surface peat and stream water in an upland catchment. *Science of the Total Environment*, 404(2), 308–315. <https://doi.org/10.1016/j.scitotenv.2007.11.002>
- Clay, G. D., & Evans, M. G. (2017). Ten-year meteorological record for an upland research catchment near the summit of Snake Pass in the Peak District, UK. *Weather*, 72(8), 242–249. <https://doi.org/10.1002/wea.2824>
- Daniels, S. M., Agnew, C. T., Allott, T. E. H., & Evans, M. G. (2008). Water table variability and runoff generation in an eroded peatland, South Pennines, UK. *Journal of Hydrology*, 361(1), 214–226. <https://doi.org/10.1016/j.jhydrol.2008.07.042>
- Daniels, S. M., Evans, M. G., Agnew, C. T., & Allott, T. E. H. (2008). Sulphur leaching from headwater catchments in an eroded peatland, South Pennines, U.K. *Science of the Total Environment*, 407(1), 481–496. <https://doi.org/10.1016/j.scitotenv.2008.08.029>
- Dupas, R., Jomaa, S., Musolff, A., Borchardt, D., & Rode, M. (2016). Disentangling the influence of hydroclimatic patterns and agricultural management on river nitrate dynamics from sub-hourly to decadal time scales. *Science of the Total Environment*, 571, 791–800. <https://doi.org/10.1016/j.scitotenv.2016.07.053>
- Edokpa, D., Milledge, D., Allott, T., Holden, J., Shuttleworth, E., Kay, M., et al. (2022). Rainfall intensity and catchment size control storm runoff in a gullied blanket peatland. *Journal of Hydrology*, 609, 127688. <https://doi.org/10.1016/j.jhydrol.2022.127688>
- Evans, M. G., Burt, T. P., Holden, J., & Adamson, J. K. (1999). Runoff generation and water table fluctuations in blanket peat: Evidence from UK data spanning the dry summer of 1995. *Journal of Hydrology*, 221(3–4), 141–160. [https://doi.org/10.1016/S0022-1694\(99\)00085-2](https://doi.org/10.1016/S0022-1694(99)00085-2)
- Flannigan, M., Stocks, B., Turetsky, M., & Wotton, M. (2009). Impacts of climate change on fire activity and fire management in the circumboreal forest. *Global Change Biology*, 15(3), 549–560. <https://doi.org/10.1111/j.1365-2486.2008.01660.x>
- Freeman, M. C., Pringle, C. M., & Jackson, C. R. (2007). Hydrologic connectivity and the contribution of stream headwaters to ecological integrity at regional scales. *Journal of the American Water Resources Association*, 43(1), 5–14. <https://doi.org/10.1111/j.1752-1688.2007.00002.x>
- Graham, A. M., Pope, R. J., McQuaid, J. B., Pringle, K. P., Arnold, S. R., Bruno, A. G., et al. (2020). Impact of the June 2018 Saddleworth Moor wildfires on air quality in northern England. *Environmental Research Communications*, 2(3), 031001. <https://doi.org/10.1088/2515-7620/ab7b92>
- Granath, G., Evans, C. D., Strengbom, J., Fölster, J., Grelle, A., Strömqvist, J., & Köhler, S. J. (2021). The impact of wildfire on biogeochemical fluxes and water quality in boreal catchments. *Biogeosciences*, 18(10), 3243–3261. <https://doi.org/10.5194/bg-18-3243-2021>
- Hampton, T. B., Lin, S., & Basu, N. B. (2022). Forest fire effects on stream water quality at continental scales: A meta-analysis. *Environmental Research Letters*, 17(6), 064003. <https://doi.org/10.1088/1748-9326/ac6a6c>
- Hamshaw, S. D., Dewoolkar, M. M., Schroth, A. W., Wemple, B. C., & Rizzo, D. M. (2018). A new machine-learning approach for classifying hysteresis in suspended-sediment discharge relationships using high-frequency monitoring data. *Water Resources Research*, 54(6), 4040–4058. <https://doi.org/10.1029/2017wr022238>
- Heathwaite, A. L., & Bieroza, M. (2021). Fingerprinting hydrological and biogeochemical drivers of freshwater quality. *Hydrological Processes*, 35(1). <https://doi.org/10.1002/hyp.13973>
- Holden, J. (2006). Chapter 14 Peatland hydrology. In *Developments in Earth surface processes* (Vol. 9, pp. 319–346). Elsevier. [https://doi.org/10.1016/S0928-2025\(06\)09014-6](https://doi.org/10.1016/S0928-2025(06)09014-6)
- Holden, J., & Burt, T. P. (2003). Hydrological studies on blanket peat: The significance of the acrotelm-catotelm model. *Journal of Ecology*, 91(1), 86–102. <https://doi.org/10.1046/j.1365-2745.2003.00748.x>
- Ivanov, K. E. (1981). *Water movement in mirelands*. Academic Press Inc. (London) Ltd.
- Jones, J. A. A. (1981). *The nature of soil piping: A review of research*. Geo Books.
- Juckers, M., & Watmough, S. A. (2014). Impacts of simulated drought on pore water chemistry of peatlands. *Environmental Pollution*, 184, 73–80. <https://doi.org/10.1016/j.envpol.2013.08.011>
- Keeley, J. E. (2009). Fire intensity, fire severity and burn severity: A brief review and suggested usage. *International Journal of Wildland Fire*, 18(1), 116. <https://doi.org/10.1071/WF07049>
- Kendon, M., McCarthy, M., Jevrejeva, S., Matthews, A., & Legg, T. (2019). State of the UK climate 2018. *International Journal of Climatology*, 39(S1), 1–55. <https://doi.org/10.1002/joc.6213>
- Kettridge, N., Turetsky, M. R., Sherwood, J. H., Thompson, D. K., Miller, C. A., Bencotter, B. W., et al. (2015). Moderate drop in water table increases peatland vulnerability to post-fire regime shift. *Scientific Reports*, 5(1), 8063. <https://doi.org/10.1038/srep08063>
- Knapp, J. L. A., Li, L., & Musolff, A. (2022). Hydrologic connectivity and source heterogeneity control concentration–discharge relationships. *Hydrological Processes*, 36(9). <https://doi.org/10.1002/hyp.14683>
- Lawler, D. M., Petts, G. E., Foster, I. D. L., & Harper, S. (2006). Turbidity dynamics during spring storm events in an urban headwater river system: The upper tame, West Midlands, UK. *The Science of the Total Environment*, 360(1–3), 109–126. <https://doi.org/10.1016/j.scitotenv.2005.08.032>
- Lawlor, A. J., & Tipping, E. (2003). Metals in bulk deposition and surface waters at two upland locations in northern England. *Environmental Pollution*, 121(2), 153–167. [https://doi.org/10.1016/S0269-7491\(02\)00228-2](https://doi.org/10.1016/S0269-7491(02)00228-2)
- Liu, W., Birgand, F., Tian, S., & Chen, C. (2021). Event-scale hysteresis metrics to reveal processes and mechanisms controlling constituent export from watersheds: A review. *Water Research*, 200, 117254. <https://doi.org/10.1016/j.watres.2021.117254>
- Lloyd, C. E. M., Freer, J. E., Johnes, P. J., & Collins, A. L. (2016). Using hysteresis analysis of high-resolution water quality monitoring data, including uncertainty, to infer controls on nutrient and sediment transfer in catchments. *Science of the Total Environment*, 543, 388–404. <https://doi.org/10.1016/j.scitotenv.2015.11.028>

- Marcotte, A. L., Limpens, J., Stoof, C. R., & Stoorvogel, J. J. (2022). Can ash from smoldering fires increase peatland soil pH? *International Journal of Wildland Fire*, 31(6), 607–620. <https://doi.org/10.1071/wf21150>
- McCarter, C. P. R., Clay, G. D., Wilkinson, S. L., Page, S., Shuttleworth, E. L., Davidson, S. J., et al. (2023). Peat fires and the unknown risk of legacy metal and metalloid pollution. *Environmental Research Letters*, 18(7), 071003. <https://doi.org/10.1088/1748-9326/acddfc>
- Miszczak, E., Stefaniak, S., Michczyński, A., Steinnes, E., & Twardowska, I. (2020). A novel approach to peatlands as archives of total cumulative spatial pollution loads from atmospheric deposition of airborne elements complementary to EMEP data: Priority pollutants (Pb, Cd, Hg). *Science of the Total Environment*, 705, 135776. <https://doi.org/10.1016/j.scitotenv.2019.135776>
- Moody, J. A., Shakesby, R. A., Robichaud, P. R., Cannon, S. H., & Martin, D. A. (2013). Current research issues related to post-wildfire runoff and erosion processes. *Earth-Science Reviews*, 122, 10–37. <https://doi.org/10.1016/j.earscirev.2013.03.004>
- Moore, P. A., Lukenbach, M. C., Kettridge, N., Petrone, R. M., Devito, K. J., & Waddington, J. M. (2017). Peatland water repellency: Importance of soil water content, moss species, and burn severity. *Journal of Hydrology*, 554, 656–665. <https://doi.org/10.1016/j.jhydrol.2017.09.036>
- Nunes, J. P., Bernard-Jannin, L., Rodríguez-Blanco, M. L., Boulet, A.-K., Santos, J. M., & Keizer, J. J. (2020). Impacts of wildfire and post-fire land management on hydrological and sediment processes in a humid Mediterranean headwater catchment. *Hydrological Processes*, 34(26), 5210–5228. <https://doi.org/10.1002/hyp.13926>
- Nunes, J. P., Doerr, S. H., Sheridan, G., Neris, J., Santín, C., Emelko, M. B., et al. (2018). Assessing water contamination risk from vegetation fires: Challenges, opportunities and a framework for progress. *Hydrological Processes*, 32(5), 687–694. <https://doi.org/10.1002/hyp.11434>
- Paul, M. J., LeDuc, S. D., Lassiter, M. G., Moorhead, L. C., Noyes, P. D., & Leibowitz, S. G. (2022). Wildfire induces changes in receiving waters: A review with considerations for water quality management. *Water Resources Research*, 58(9), e2021WR030699. <https://doi.org/10.1029/2021WR030699>
- Pereira, P., Úbeda, X., & Martin, D. A. (2012). Fire severity effects on ash chemical composition and water-extractable elements. *Geoderma*, 191, 105–114. <https://doi.org/10.1016/j.geoderma.2012.02.005>
- Perry, M. C., Vanvyve, E., Betts, R. A., & Palin, E. J. (2022). Past and future trends in fire weather for the UK. *Natural Hazards and Earth System Sciences*, 22(2), 559–575. <https://doi.org/10.5194/nhess-22-559-2022>
- R core team. (2022). R statistical software (version 4.2.1).
- Robinne, F.-N., Hallema, D. W., Bladon, K. D., Flannigan, M. D., Boisramé, G., Bréthaut, C. M., et al. (2021). Scientists' warning on extreme wildfire risks to water supply. *Hydrological Processes*, 35(5), e14086. <https://doi.org/10.1002/hyp.14086>
- Rothwell, J. J., Evans, M. G., & Allott, T. E. H. (2007). Lead contamination of fluvial sediments in an eroding blanket peat catchment. *Applied Geochemistry*, 22(2), 446–459. <https://doi.org/10.1016/j.apgeochem.2006.11.002>
- Rothwell, J. J., Evans, M. G., Daniels, S. M., & Allott, T. E. H. (2007). Baseflow and stormflow metal concentrations in streams draining contaminated peat moorlands in the Peak District National Park (UK). *Journal of Hydrology*, 341(1–2), 90–104. <https://doi.org/10.1016/j.jhydrol.2007.05.004>
- Rothwell, J. J., Robinson, S. G., Evans, M. G., Yang, J., & Allott, T. E. H. (2005). Heavy metal release by peat erosion in the Peak District, southern Pennines, UK. *Hydrological Processes*, 19(15), 2973–2989. <https://doi.org/10.1002/hyp.5811>
- Rozemeijer, J. C., van der Velde, Y., van Geer, F. C., de Rooij, G. H., Torts, P. J. J. F., & Broers, H. P. (2010). Improving load estimates for NO₃ and P in surface waters by characterizing the concentration response to rainfall events. *Environmental Science & Technology*, 44(16), 6305–6312. <https://doi.org/10.1021/es101252e>
- Rust, A. J., Saxe, S., McCray, J., Rhoades, C. C., & Hogue, T. S. (2019). Evaluating the factors responsible for post-fire water quality response in forests of the western USA. *International Journal of Wildland Fire*, 28(10), 769. <https://doi.org/10.1071/WF18191>
- Sánchez-García, C., Santín, C., Neris, J., Sigmund, G., Otero, X. L., Manley, J., et al. (2023). Chemical characteristics of wildfire ash across the globe and their environmental and socio-economic implications. *Environment International*, 178, 108065. <https://doi.org/10.1016/j.envint.2023.108065>
- Santín, C., Doerr, S. H., Otero, X. L., & Chafer, C. J. (2015). Quantity, composition and water contamination potential of ash produced under different wildfire severities. *Environmental Research*, 142, 297–308. <https://doi.org/10.1016/j.envres.2015.06.041>
- Shakesby, R., & Doerr, S. (2006). Wildfire as a hydrological and geomorphological agent. *Earth-Science Reviews*, 74(3–4), 269–307. <https://doi.org/10.1016/j.earscirev.2005.10.006>
- Shotbolt, L., Hutchinson, S. M., & Thomas, A. D. (2006). Sediment stratigraphy and heavy metal fluxes to reservoirs in the Southern Pennine Uplands, UK. *Journal of Paleolimnology*, 35(2), 305–322. <https://doi.org/10.1007/s10933-005-1594-2>
- Shuttleworth, E. L., Clay, G. D., Evans, M. G., Hutchinson, S. M., & Rothwell, J. J. (2017). Contaminated sediment dynamics in Peatland headwater catchments. *Journal of Soils and Sediments*, 17(11), 2637–2647. <https://doi.org/10.1007/s11368-017-1674-8>
- Shuttleworth, E. L., Evans, M. G., Hutchinson, S. M., & Rothwell, J. J. (2014). Assessment of lead contamination in Peatlands using field portable XRF. *Water, Air, and Soil Pollution*, 225(2), 1844. <https://doi.org/10.1007/s11270-013-1844-2>
- Shuttleworth, E. L., Evans, M. G., Hutchinson, S. M., & Rothwell, J. J. (2015). Peatland restoration: Controls on sediment production and reductions in carbon and pollutant export. *Earth Surface Processes and Landforms*, 40(4), 459–472. <https://doi.org/10.1002/esp.3645>
- Shuttleworth, E. L., Evans, M. G., Pilkington, M., Spencer, T., Walker, J., Milledge, D., & Allott, T. E. H. (2019). Restoration of blanket peat moorland delays stormflow from hillslopes and reduces peak discharge. *Journal of Hydrology*, 2, 100006. <https://doi.org/10.1016/j.jhydro.2018.100006>
- Smith, H. G., Sheridan, G. J., Lane, P. N. J., Nyman, P., & Haydon, S. (2011). Wildfire effects on water quality in forest catchments: A review with implications for water supply. *Journal of Hydrology*, 396(1), 170–192. <https://doi.org/10.1016/j.jhydrol.2010.10.043>
- Stirling, E., Fitzpatrick, R. W., & Mosley, L. M. (2020). Drought effects on wet soils in inland wetlands and peatlands. *Earth-Science Reviews*, 210, 103387. <https://doi.org/10.1016/j.earscirev.2020.103387>
- Swindle, C., Shankin-Clarke, P., Meyerhof, M., Carlson, J., & Melack, J. (2021). Effects of wildfires and ash leaching on stream chemistry in the Santa Ynez Mountains of Southern California. *Water*, 13(17), 2402. <https://doi.org/10.3390/w13172402>
- Szkokan-Emilson, E. J., Kielstra, B., Watmough, S., & Gunn, J. (2013). Drought-induced release of metals from peatlands in watersheds recovering from historical metal and sulphur deposition. *Biogeochemistry*, 116(1–3), 131–145. <https://doi.org/10.1007/s10533-013-9919-0>
- Tetzlaff, D., Buttle, J., Carey, S. K., McGuire, K., Laudon, H., & Soulsby, C. (2015). Tracer-based assessment of flow paths, storage and runoff generation in northern catchments: A review. *Hydrological Processes*, 29(16), 3475–3490. <https://doi.org/10.1002/hyp.10412>
- Tiwari, T., Sponseller, R. A., & Laudon, H. (2022). The emerging role of drought as a regulator of dissolved organic carbon in boreal landscapes. *Nature Communications*, 13(1), 5125. <https://doi.org/10.1038/s41467-022-32839-3>
- Twardowska, I., & Kyzioł, J. (2003). Sorption of metals onto natural organic matter as a function of complexation and adsorbent-adsorbate contact mode. *Environment International*, 28(8), 783–791. [https://doi.org/10.1016/S0160-4120\(02\)00106-X](https://doi.org/10.1016/S0160-4120(02)00106-X)

- van Meerveld, H. J. I., Kirchner, J. W., Vis, M. J. P., Assendelft, R. S., & Seibert, J. (2019). Expansion and contraction of the flowing stream network alter hillslope flowpath lengths and the shape of the travel time distribution. *Hydrology and Earth System Sciences*, 23(11), 4825–4834. <https://doi.org/10.5194/hess-23-4825-2019>
- Waddington, J. M., Morris, P. J., Kettridge, N., Granath, G., Thompson, D. K., & Moore, P. A. (2015). Hydrological feedbacks in northern peatlands. *Ecohydrology*, 8(1), 113–127. <https://doi.org/10.1002/eco.1493>
- Wilkinson, S. L., Andersen, R., Moore, P. A., Davidson, S. J., Granath, G., & Waddington, J. M. (2023). Wildfire and degradation accelerate northern peatland carbon release. *Nature Climate Change*, 13(5), 456–461. <https://doi.org/10.1038/s41558-023-01657-w>
- Wilkinson, S. L., Tekatch, A. M., Markle, C. E., Moore, P. A., & Waddington, J. M. (2020). Shallow peat is most vulnerable to high peat burn severity during wildfire. *Environmental Research Letters*, 15(10), 104032. <https://doi.org/10.1088/1748-9326/aba7e8>
- Wolverson-Cope, F. (1976). *Geology Explained in the peak district*. Devon: David and Charles.
- Worrall, F., Burt, T., & Adamson, J. (2003). Controls on the chemistry of runoff from an upland peat catchment. *Hydrological Processes*, 17(10), 2063–2083. <https://doi.org/10.1002/hyp.1244>
- Wu, Y., Zhang, N., Slater, G., Waddington, J. M., & de Lannoy, C.-F. (2020). Hydrophobicity of peat soils: Characterization of organic compound changes associated with heat-induced water repellency. *Science of the Total Environment*, 714, 136444. <https://doi.org/10.1016/j.scitotenv.2019.136444>
- Xu, J., Morris, P. J., Liu, J., & Holden, J. (2018). PEATMAP: Refining estimates of global peatland distribution based on a meta-analysis. *Catena*, 160, 134–140. <https://doi.org/10.1016/j.catena.2017.09.010>
- Zuecco, G., Penna, D., Borga, M., & van Meerveld, H. J. (2016). A versatile index to characterize hysteresis between hydrological variables at the runoff event timescale. *Hydrological Processes*, 30(9), 1449–1466. <https://doi.org/10.1002/hyp.10681>